Vibrational spectroscopic studies, Fukui functions, HOMO-LUMO, NLO, NBO analysis and molecular docking study of (E)-1-(1,3-benzodioxol-5-yl)-4,4-dimethylpent-1-en-3-one, a potential precursor to bioactive agents

Reference:
Al-Wabli Reem I., Resmi K. S., Mary Y. Sheena, Panicker C. Yohannan, Attia Mohamed I., El-Emam Ali A., Van Alsenoy Christian.- Vibrational spectroscopic studies, Fukui functions, HOMO-LUMO, NLO, NBO analysis and molecular docking study of (E)-1-(1,3-benzodioxol-5-yl)-4,4-dimethylpent-1-en-3-one, a potential precursor to bioactive agents
Journal of molecular structure - ISSN 0022-2860 - 1123(2016), p. 375-383
Full text (Publisher's DOI): https://doi.org/10.1016/J.MOLSTRUC.2016.07.044
To cite this reference: https://hdl.handle.net/10067/1356930151162165141

Accepted Manuscript

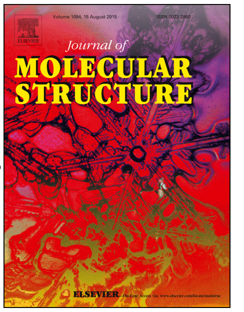

Vibrational spectroscopic studies, Fukui functions, HOMO-LUMO, NLO, NBO analysis and molecular docking study of (E)-1-(1,3-benzodioxol-5-yl)-4,4-dimethylpent-1-en-3-one, a potential precursor to bioactive agents

Reem I. Al-Wabli, K.S. Resmi, Y. Sheena Mary, C. Yohannan Panicker, Mohamed A. Attia, Ali A. El-Emam, C. Van Alsenoy

PII: S0022-2860(16)30725-6

DOI: 10.1016/j.molstruc.2016.07.044

Reference: MOLSTR 22747

To appear in: *Journal of Molecular Structure*

Received Date: 6 March 2016

Accepted Date: 12 July 2016

Please cite this article as: R.I. Al-Wabli, K.S. Resmi, Y. Sheena Mary, C. Yohannan Panicker, M.A. Attia, A.A. El-Emam, C. Van Alsenoy, Vibrational spectroscopic studies, Fukui functions, HOMO-LUMO, NLO, NBO analysis and molecular docking study of (E)-1-(1,3-benzodioxol-5-yl)-4,4-dimethylpent-1-en-3-one, a potential precursor to bioactive agents, *Journal of Molecular Structure* (2016), doi: 10.1016/ j.molstruc.2016.07.044.

Graphical abstract

Title of the paper: Vibrational spectroscopic studies, Fukui functions, HOMO-LUMO, NLO, NBO analysis and molecular docking study of (E)-1-(1,3-benzodioxol-5-yl)-4,4-dimethylpent-1-en-3-one, a potential precursor to bioactive agents

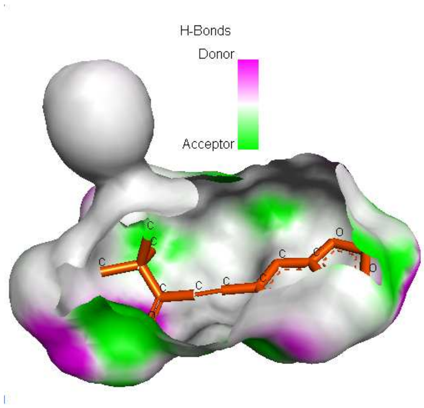

Vibrational spectroscopic studies, Fukui functions, HOMO-LUMO, NLO, NBO analysis and molecular docking study of (E)-1-(1,3-benzodioxol-5-yl)-4,4-dimethylpent-1-en-3-one, a potential precursor to bioactive agents

Reem I. Al-Wabli[a], K.S.Resmi[b], Sheena Mary Y[c], C.Yohannan Panicker[c*], Mohamed A. Attia[a,d], Ali A. El-Emam[a], C.Van Alsenoy[e]

[a] Department of Pharmaceutical Chemistry, College of Pharmacy, King Saud University, Riyadh 11451,Saudi Arabia

Department of Physics, TKM College of Arts and Science, Kollam, Kerala, India

[c]Department of Physics, Fatima Mata National College, Kollam, Kerala, India

[d] Pharmaceutical and Drug Industries Research Division, Department of Medicinal and Pharmaceutical Chemistry, National Research Centre, Dokki, Giza 12622, Egypt

[e]Department of Chemistry, University of Antwerp, Groenenborgerlaan 171, B-2020 Antwerp, Belgium

*author for correspondence:email:cyphyp@rediffmail.com

ABSTRACT

The FT-IR and FT-Raman spectra of (E)-1-(1,3-benzodioxol-5-yl)-4,4-dimethylpent-1-en-3-one were recorded and analyzed experimentally and theoretically. The observed experimental and theoretical wavenumbers were assigned using potential energy distribution. The NLO properties were evaluated by the determination of first and second hyperpolarizabilities of the title compound. From the frontier molecular orbital study, the HOMO centers over the entire molecule except the methyl groups, while the LUMO is over the entire molecule except the CH_2 group with the dioxole ring and one of the methyl groups. From the MEP plot, it is evident that the negative region covers the carbonyl and C=C groups and the positive region is over CH_2 groups. The Fukui functions are also reported. The calculated geometrical parameters are in agreement with the XRD results. From the molecular docking study, the docked ligand title compound forms a stable complex with the androgen receptor and gives a binding affinity value of -8.1 kcal/mol and the results suggest that the compound might exhibit inhibitory activity against androgen receptor.

Keywords: DFT; benzodioxole; FT-IR; FT-Raman; Molecular docking.

1. Introduction

1,3-Benzodioxole moiety constitutes an essential structure motif in several naturally-occurring [1-5] bioactive compounds. In addition, a considerable number of biomolecules having 1,3-bezodioxole moiety display multifarious biological activities including anticonvulsant [6-8], anti-depressant [9], anticancer [10,11], immunomodulatory [12] and antiprotozoal [13] activities. The title compound, (*E*)-1-(1,3-benzodioxol-5-yl)-4,4-dimethylpent-1-en-3-one, is the precursor of the anticonvulsant orphan drug, stiripentol which was clinically approved as anticonvulsant drug [14]. The molecular conformations of indan-like benzene fused ring molecules including 1,3-benzodioxole derivatives have been exclusively studied due to their interesting conformational properties [15-21]. Fun et al. [22] reported the single crystal XRD study of the title compound. In the present study, the IR and Raman spectra of the title compound are reported both experimentally and theoretically. In addition, the NBO analysis, molecular electrostatic potential and nonlinear optical properties are reported. The molecular docking studies are also reported due to the diverse biological activities of 1,3-benzodioxole derivatives.

2. Experimental details

The title compound was prepared via condensation of equimolar amounts of piperonal and pinacolone in aqueous methanolic potassium hydroxide at 70 ^{o}C for five hours [8]. The FT-IR spectrum (Fig. 1) was recorded using KBr pellets on a DR/Jasco FT-IR 6300 spectrometer with a spectral resolution of 2 cm^{-1}. The FT-Raman spectrum (Fig. 2) was obtained on a Bruker RFS 100/s, Germany, and for excitation of the spectrum, the emission of Nd:YAG laser was used, excitation wavelength was 1064 nm, maximal power was 150 mW and measurement was carried out on solid sample.

3. Computational details

All calculations have been performed with the Gaussian09 program package using the density functional theoretical method (DFT) with Becke-3-Lee-Yang-Parr (B3LYP) combined with the standard basis set SDD (6D, 10F) [23] and since the DFT method tends to overestimate the fundamental modes, a scaling factor of 0.9613 has to be used for obtaining a considerable better agreement with the experimental data [24, 25]. The Stuttgart/Dresden effective core potential basis set (SDD) [26] was chosen particularly because of its advantage of doing faster calculations with relatively better accuracy and structures [27]. The parameters corresponding to the optimized geometry (Fig. 3) of the title compound with the experimental XRD data [22] are given Table S1 (supporting material). The assignments of the calculated wavenumbers are aided by the Gaussview program [28] and potential energy distribution analysis [29].

4. Results and discussion

4.1 Geometrical parameters

For the title compound, the carbon-carbon bond lengths (DFT/XRD) in the phenyl ring lies in the range 1.3891-1.4301/1.3668-1.4125 Å and the bond lengths are somewhere in between the normal values for a single (1.54 Å) and a double (1.33 Å) bond [30]. The bond length (DFT/XRD) C_9-C_{10} is longer (1.4301/1.4125 Å) due to the presence of adjacent C=C group. The C-O bond lengths (DFT/XRD) lie in the range 1.4058-1.4803/1.3685-1.4378 Å which are in agreement with literature [31]. For the title compound, the bond lengths (DFT/XRD) C_{14}-C_{15} = 1.5450/1.5262, C_{14}-C_{28} = 1.5570/1.5363, C_{14}-C_{16} = 1.5570/1.5363, C_{13}-C_{14} = 1.5482/1.5298 Å and these high values are attributed to the presence of the adjacent methyl groups [31]. For the title compound, the C=O and C=C bond lengths (DFT/XRD) are 1.2596/1.2214 and 1.3611/1.3465 Å, respectively, which are in agreement with reported values [31, 32]. At C_6 and C_8, the bond angles (DFT/XRD) are C_5-C_6-C_8 = 121.6/121.9˚, C_5-C_6-O_1 = 128.0/128.2˚, C_8-C_6-O_1 = 110.3/109.8˚, C_6-C_8-C_9 = 122.4/122.4˚, C_6-C_8-O_2 = 110.0/109.8˚ and C_9-C_8-O_2 = 127.6/127.7˚ and this asymmetry in angles are due to the hydrogen bonding in the molecule as reported in literature [22]. At C_{10} and C_{13} positions, the bond angles (DFT/XRD) are C_4-C_{10}-C_9 = 119.4/119.5˚, C_4-C_{10}-C_{11} = 118.1/119.0˚, C_9-C_{10}-C_{11} = 122.4/121.4˚, C_{14}-C_{13}-C_{12} = 118.1/117.4˚, C_{14}-C_{13}-O_3 = 121.1/121.6˚ and C_{12}-C_{13}-O_3 = 120.8/120.9˚, and the asymmetry in the angles are due to the presence of adjacent groups. The phenyl and 1,3-dioxole rings are planar as is evident from the torsion angles, C_5-C_6-O_1-C_7, C_5-C_6-C_8-O_2, C_9-C_8-O_2-C_7 and C_9-C_8-C_6-O_1 (Table S1).

4.2 IR and Raman spectra

The observed IR, Raman bands, calculated (scaled wavenumbers) and assignments are given in Table 1. The CH stretching modes of the phenyl ring are theoretically assigned at 3126, 3123 and 3089 cm^{-1} for the title compound [33] and only one band is observed in the Raman spectrum at 3124 cm^{-1}. For tri-substituted phenyl ring the ring stretching modes are expected in the region 1640-1250 cm^{-1} [33] and these modes are assigned at 1605, 1585 cm^{-1} in the IR spectrum, 1595, 1419 cm^{-1} in the Raman spectrum and theoretically at 1599, 1581, 1463, 1425, 1359 cm^{-1}. In asymmetric tri-substituted benzenes, the wavenumber interval of the ring breathing mode is expected at 500-600 cm^{-1} when all the three substituents are light [33, 34]. When all the three substituents are heavy, the ring breathing mode wavenumber appears above 1100 cm^{-1} and in the case of mixed substituent the wavenumber is expected to appear between 600 and 750 cm^{-1}. For the title compound, the ring breathing mode of the phenyl ring is theoretically assigned at 769 cm^{-1} and bands are observed at 764 cm^{-1} in the IR spectrum and at 766 cm^{-1} in the Raman spectra, respectively. The ring breathing mode of a tri-substituted phenyl ring is theoretically reported at 796 cm^{-1} by Panicker et al. [18] and at 733 (IR), 738 cm^{-1} by Mary et al. [35]. The in-plane and out-of-plane CH deformation modes of the phenyl ring are expected above and below 1000 cm^{-1} [33]. In the present case, the bands at

1258, 1120 (IR), 1256 (Raman), 1254, 1180, 1117 cm^{-1} (DFT) and 882, 830 (IR), 951, 828 (Raman), 949, 880, 824 cm^{-1} (DFT) are assigned as the CH in-plane and out-of-plane deformations of the phenyl ring, respectively.

The asymmetric and symmetric C-O-C stretching modes are expected in the region 1250-850 cm^{-1} [33]. The C-O-C stretching modes are reported at 1224, 1160, 1046, 1027 (DFT), 1171, 1066, 1036 (IR), 1051, 1028 cm^{-1} (Raman) for 1,3-benzodioxole [18] and at 1250, 1073 cm^{-1} [36], 1263, 1055 cm^{-1} [37]. For the title compound, the C-O-C stretching modes are observed at 1045, 977 cm^{-1} in the IR spectrum, 1045, 860 cm^{-1} in the Raman spectrum and theoretically at 1047, 974, 863, 850 cm^{-1}.

The stretching vibrations of the CH_2 group (the asymmetric and symmetric stretch) and the deformation modes (scissoring, wagging, twisting and rocking modes) are expected in the regions 3050-2850 and 1480-800 cm^{-1}, respectively [33,38]. The CH_2 stretching modes are assigned at 2976 cm^{-1} in the IR spectrum, 2973 cm^{-1} in the Raman spectrum and at 3056, 2979 cm^{-1} theoretically. The CH_2 deformation modes are assigned at 1475, 1354, 1116 and 1059 cm^{-1} theoretically for the title compound as expected [33].

The CH_3 stretching modes are expected in the region 2900-3050 cm^{-1} [33]. The bands observed at 3020, 2921 cm^{-1} in the IR spectrum, 3018, 2922 cm^{-1} in the Raman spectrum and in the range 3030-2920 cm^{-1} (DFT) are assigned as the stretching modes of the methyl group. The methyl asymmetrical deformations are expected in the region 1460±15 and the symmetrical deformations at 1350±20 cm^{-1} [33]. The DFT calculation gives these deformations in the ranges 1479-1442 and 1398-1371 cm^{-1} as asymmetric and symmetric deformation modes for the title compound. The deformation modes are observed experimentally at 1481, 1450, 1396, 1369 cm^{-1} in the IR spectrum and at 1482, 1450, 1370 cm^{-1} in the Raman spectrum for the title compound. The methyl rocking vibration has been expected at 1050±30 and 950±40 cm^{-1} [33]. The bands observed at 939 cm^{-1} in the IR spectrum, 940 cm^{-1} in the Raman spectrum and in the range 1004-911cm^{-1} (DFT) are assigned as the methyl rocking modes.

The tertiary butyl group $C(CH_3)_3$ gives rise to five skeletal deformations absorbing in the three regions: $\delta_{as}CC_3$ in 435±85, δ_sCC_3 in 335±80 and ρCC_3 in 300±80 cm^{-1} [33]. The highest (lowest) values for $\delta_{as}CC_3$ are observed around 510 (355) cm^{-1} [30]. Most of the $\delta_{as}CC_3$ modes have been assigned in the region 435±65 cm^{-1} [33]. The DFT calculations give the values 560, 368 and 368 cm^{-1} as asymmetric and symmetric deformations. The bands at 340 and 293 cm^{-1} (DFT) are assigned as the rocking modes of the CC_3. The torsion modes τCH_3 and τCC_3 are expected in the low frequency region [33]. The $\upsilon_{as}CC_3$ and υ_sCC_3 modes are expected in the regions 1235±60 and 800±90 cm^{-1}, respectively [33]. For the title compound, the bands observed at 1240 cm^{-1} in the IR spectrum and theoretically at 1239, 1204 cm^{-1} are assigned as the $\upsilon_{as}CC_3$ modes. The DFT calculations give the symmetric υ_sCC_3 stretching mode at 791 cm^{-1} and the band observed at 792 cm^{-1} in the IR spectrum are assigned as these modes.

According to Socrates [39], the C=C stretching mode is expected around 1600 cm^{-1} when conjugated with the C=O group. For the title compound, the band observed at 1523 in the IR spectrum, 1540 in the Raman spectrum and theoretically at 1535 cm^{-1} is assigned as the C=C stretching mode and the C=O stretching mode is observed at 1624 cm^{-1} in the Raman spectrum and theoretically at 1625 cm^{-1}. For the title compound, the CH modes associated with the anhyride group are assigned at 3085, 1308, 1222, 1018 cm^{-1} in the IR spectrum, 1308, 1019 cm^{-1} in the Raman spectrum and theoretically at 3087, 3052, 1309, 1225, 1020, 892 cm^{-1}. The root mean square value between the calculated and observed wavenumbers were calculated inorder to investigate the performance of the vibrational wavenumbers of the title compound and the RMS errors are 3.17 for IR bands and 3.39 for Raman bands.

4.3 Nonlinear optical properties (NLO)

Dipole moment, polarizability and hyperpolarizabilities of organic molecules are important response properties. There has been an intense investigation for molecules with large non-zero hyperpolarizabilities, since these substances have potential as the constituents of nonlinear optical materials. According to the present calculations, the first static hyperpolarizability calculated β value is found to be 30.75×10^{-30}e.s.u which is 236.54 times that of standard NLO material urea (0.13×10^{-30}e.s.u) [40]. The average second hyperpolarizability is $\langle\gamma\rangle = (\gamma_{xxxx} + \gamma_{yyyy} + \gamma_{zzzz} + 2\gamma_{xxyy} + 2\gamma_{xxzz} + 2\gamma_{yyzz})/5$. The theoretical second order hyperpolarizability was calculated using the Gaussian09 software and is equal to -14.39×10^{-37}e.s.u [41]. We conclude that the title compound is an attractive object for future studies of nonlinear optical properties.

4.4 Frontier molecular orbital analysis

The frontier orbital electron densities of atoms can be used as an efficient tool for the detailed characterization of donor acceptor interactions [42]. The HOMO and LUMO energies are calculated at the B3LYP/SDD level and the orbitals energy diagrams are shown in Fig. 4. As can be clearly seen from Fig. 4, the HOMO is over the entire molecule except the methyl groups, while the LUMO is over the entire molecule except the CH_2 group with the dioxole ring and one of the methyl groups. The chemical reactivity descriptors like chemical potential, hardness and electrophilicity index are proposed for understanding various aspects of pharmacological sciences including drug design and possible eco-toxicological characteristics of the drugs. Using the HOMO and LUMO orbital energies, the ionization energy and electron affinity can be expressed as: $I = -E_{HOMO}$, $A = -E_{LUMO}$ [43]. The hardness η and chemical potential μ are given the following relations $\eta = (I-A)/2$ and $\mu = -(I+A)/2$, where I and A are the first ionization potential and electron affinity of the chemical species [43]. For the title compound, the E_{HOMO} = -7.822 eV, E_{LUMO} = -5.770 eV, Energy gap = HOMO-LUMO = 2.052 eV, Ionization potential I = 7.822 eV, Electron affinity A = 5.770 eV, global hardness η = 1.026 eV, chemical potential μ = -6.796 eV, global electrophiliciy = $\mu^2/2\eta$ = 22.51 eV. It is indicative that the chemical potential of the title compound is negative and it means that the compound is stable.

4.5 Molecular electrostatic potential (MEP)

The molecular electrostatic potential map yields information on the molecular regions those are preferred or avoided by an electrophile or nucleophile. Any chemical system creates an electrostatic potential around itself, when a hypothetical volumeless unit positive charge is used as a probe, the probe feels the attractive or repulsive forces in regions where the electrostatic potential is negative or positive, respectively [31]. Molecular electrostatic potential is found to be a very useful tool in the investigation of the correlation between the molecular structure and the physiochemical property relationship of the molecules including biomolecules and drugs [44-49] and it provides a visual method to understand the relative polarity of the molecule and the different values of the electrostatic potential is represented by different colors; red, blue and green represent regions of most negative, most positive and zero electrostatic potential, respectively. The negative (red and yellow) regions of the MEP were related to electrophilic reactivity and the positive (blue) regions to nucleophilic reactivity. From the MEP plot (Fig. 5), it is evident that the negative region covers the carbonyl and C=C groups and the positive region is over CH_2 groups.

4.6 Fukui functions

The Fukui function is a local reactivity descriptor which gives the preferred regions where a chemical species will change its density when the number of electrons is modified. Hence, these descriptors indicate the propensity of the electronic density to deform at a given position upon accepting or donating electrons [50-52]. Also, it is possible to define the corresponding condensed or atomic Fukui functions on the j^{th} atom site as,

$f_j^- = q_j(N) - q_j(N-1)$

$f_j^+ = q_j(N+1) - q_j(N)$

$f_j^0 = ½[q_j(N+1) - q_j(N-1)]$

For an electrophilic $f_j^{-}(r)$, nucleophilic or free radical attack $f_j^{+}(r)$, on the reference molecule, respectively. In these equations, q_j is the atomic charge (evaluated from Mulliken population analysis, electrostatic derived charge, etc.) at the j^{th} atomic site is the neutral (N), anionic (N + 1) or cationic (N - 1) chemical species. Morell *et al.*, [53] have recently proposed a dual descriptor ($\Delta f(r)$), which is defined as the difference between the nucleophilic and electrophilic Fukui function and is given by, $\Delta f(r) = [f^{+}(r) - f^{-}(r)]$

$\Delta f(r) > 0$, then the site is favored for a nucleophilic attack, whereas if $\Delta f(r) < 0$, then the site may be favored for an electrophilic attack. The dual descriptors $\Delta f(r)$ give a clear difference between nucleophilic and electrophilic attack at a particular site with their sign and it provide positive value for site prone for nucleophilic attack and a negative value prone for electrophilic attack. From the values reported in Table S2(supporting material), according to the condition for dual descriptor, nucleophilic site for in our title compound is O1, O2, C4, C5, C8, C10, C12, C14, C15, C16, H17, H18, H19, H20, C28, H29 (positive value i.e. $\Delta f(r) > 0$). Similarly the electrophilic attack site is O3, C6, C7, C9, C11, C13, H21, H22, H23, H24, H25, H26, H27, H30, H31, H32, H33(negative value i.e. $\Delta f(r) < 0$). The behavior of molecules as electrophiles/nucleophiles during reaction depends on the local behavior of molecules.

4.7 Natural bond orbital analysis

The natural bond orbitals (NBO) calculations were performed using the NBO 3.1 program [54] as implemented in the Gaussian09 package at the DFT/B3LYP level and the important results are tabulated in Tables 2 and 3. The important intra-molecular hyper-conjugative interactions are: $n_2(O_1)\rightarrow\pi^*(C_5\text{-}C_6)$, $n_2(O_2)\rightarrow\pi^*(C_8\text{-}C_9)$ and $n_2(O_3)\rightarrow\sigma^*(C_{13}\text{-}C_{14})$ with stabilization energies 28.81, 27.81 and 21.20 KJ/mol with electron densities 0.37275e, 0.34340e and 0.07527e. The natural hybrid orbitals with lower energies and high occupation numbers are : $n_1(O_1)$, $n_1(O_{372})$ and $n_1(O_3)$ with energies, -0.60055, -0.59875, -0.66104 a.u and p-characters, 57.66, 57.45, 43.63% and high occupation numbers, 1.96172, 1.96105, 1.97714 while the orbitals with higher energies and low occupation numbers are: $n_2(O_1)$, $n_2(O_2)$ and $n_2(O_3)$ with energies, -0.33106, -0.32875, -0.24018 a.u and considerable p-characters of 100% and low occupation numbers, 1.84600, 1.85769 and 1.88474. Thus, a very close to pure p-type lone pair orbital participates in the electron donation to the $n_2(O_1)\rightarrow\pi^*(C_5\text{-}C_6)$, $n_2(O_2)\rightarrow\pi^*(C_8\text{-}C_9)$ and $n_2(O_3)\rightarrow\sigma^*(C_{13}\text{-}C_{14})$ interactions in the compound.

4.8 Molecular docking

Androgens (ARs) play an important role in the growth of prostate cancer and normal prostate. Prostate cancer represents the most common male malignancy [55]. Curcumin analogues were evaluated as potential androgen receptor antagonists against two human prostate cancer cell lines, PC-3 and DU-145 [56]. ARs and androgen-dependent and independent signaling pathways has occurred in the context of prostate cancer. However, AR as a therapeutic target should be explored in other tumors [57, 58]. 1,3-Dioxol derivatives were reported to exhibits anti-cancer activity against breast cancer cells T47D [59]. High resolution crystal structure of androgen receptor was downloaded from the protein data bank website (PDB ID: 1GS4) and all molecular docking calculations were performed on AutoDock-Vina software [60] and the 3D crystal structure of androgen receptor was obtained from Protein Data Bank and the protein was prepared for docking by removing the co-crystallized ligands, waters and co-factors. The Auto Dock Tools (ADT) graphical user interface was used to calculate Kollman charges and polar hydrogens and the ligand was prepared for docking by minimizing its energy at the B3LYP/SDD (6D, 10F) level of theory and the partial charges were calculated by the Geistenger method. The active site of the enzyme was defined to include the residues of the active site within the grid size of 40 Å × 40 Å × 40 Å and the most popular algorithm, Lamarckian Genetic Algorithm (LGA) available in Autodock was employed for docking.· The docking protocol was tested by extracting the co-crystallized inhibitor from the protein and then docking the same and the docking protocol predicted the same conformation as was present in the crystal structure with RMSD value well within the reliable range of 2 Å [61]. Amongst the docked conformations, the one which binds well at the active site was analyzed for detailed interactions in Discover Studio Visualizer 4.0 software. The ligand binds at the active site of the substrate (Figs. 6 and 7) by weak non-covalent interactions. His701 amino acid form H-bond with the C=O group and the amino acids Gln711, Met745 shows H-bond interaction with the dioxole ring. Phe764 amino acid indicates π-π interaction with the dioxol and phenyl rings. The amino acids Ala877, Met780, Leu873, Leu880, His701 and Phe876 form alkyl interaction with the CH_3 groups. Leu707, Met745, Met749 shows π-alkyl interaction with the dioxol and phenyl rings. The docked ligand title compound forms a stable complex with the androgen receptor (Fig. 8) and gives a binding affinity (ΔG in kcal/mol) value of -8.1 (Table 4). These preliminary results suggest that the compound might exhibit inhibitory activity against androgen receptor.

5. Conclusions

FT-IR and FT-Raman spectra of (*E*)-1-(1,3-benzodioxol-5-yl)-4,4-dimethylpent-1-en-3-one were recorded and analyzed. The vibrational wavenumbers were computed using DFT quantum chemical calculations and the data obtained from wavenumber calculations were used to assign the vibrational bands obtained experimentally. A detailed molecular picture of the title compound and its interactions were obtained from NBO and frontier molecular orbital analysis. The first and second order hyperpolarizability values are calculated and the first static hyperpolarizability is found to be 236.54 times that of standard NLO material urea and hence the title compound and its derivatives are good object for further studies in nonlinear optics. From the molecular docking study, the ligand binds at the active site of the substrate by weak non-covalent interactions: His701 amino acid form H-bond with the C=O group and the amino acids Gln711, Met745 shows H-bond interaction with the dioxole ring. Phe764 amino acid indicates π-π interaction with the dioxol and phenyl rings and the amino acids Ala877, Met780, Leu873, Leu880, His701 and Phe876 form alkyl interaction with the CH_3 groups and Leu707, Met745, Met749 shows π-alkyl interaction with the dioxol and phenyl rings. The geometrical parameters theoretically obtained are in good agreement with the reported XRD data.

Acknowledgements

The authors would like to extend their sincere appreciation to the Deanship of Scientific Research at King Saud University for funding this work through the Research Group Project No. RGP-VPP-196. The authors are thankful to University of Antwerp for access to the University's CalcUA Supercomputer Cluster.

References

[1] M. Yanagisawa, H. Kurihara, S. Kimura, Y. Tomobe, M. Kobayashi, Y. Mitsui, Y. Yazaki, K. Goto, T. Masaki, Nature 332 (1988) 411.

[2] B.S. Siddiqui, T. Gulzar, A. Mahmood, S. Begum, B. Khan, F. Afshan, Chem. Pharm. Bull. 52 (2004) 1349.

[3] M.H. Mehmood, A.H. Gilani, J. Med. Food 13 (2010) 1086.

[4] S.A. Sudjarwo, Folia Medica Indonesiana, 41 (2005) 190.

[5] V. Diwan, H. Poudyal, L. Brown, Cell Biochem. Biophys. 67 (2013) 297.

[6] M.E. Pedersen, B. Metzler, G.I. Stafford, J. van Staden, A.K. Jäger, H.B. Rasmussen, Molecules 14 (2009) 3833.

[7] M.K. Trojnar, K. Wojtal, M.P. Trojnar, S.J. Czuczwar, Pharmacol. Rep. 57 (2005) 154.

[8] M.N. Aboul-Enein, A.A. El-Azzouny, M.I. Attia, Y.A. Maklad, K.M. Amin, M. Abdel-Rehim, M.F. El-Behairy, Eur. J. Med. Chem. 47 (2012) 360.

[9] S. Li, C. Wang, M. Wang, W. Li, K. Matsumoto, Y. Tang, Life Sci. 80 (2007) 1373.

[10] N. Micale, M. Zappala, S. Grasso, Il Farmaco 58 (2003) 351.

[11] A.C.L. Leite, K.P. da Silva, I.A. de Souza, J.M. de Araujo, ´D.J. Brondani, Eur. J. Med. Chem. 39 (2004) 1059.

[12] D.P. Bezerra, F.O. de Castro, A.P.N. Alves, C. Pessoa, M.O. de Moraes, E.R. Silveira, M.A. Lima, F.J. Elmiro, N.M. de Alencar, R.O. Mesquita, M.W. Lima, L.V. Costa-Lotufo, J. Appl. Toxicol. 28 (2008) 156.

[13] L.O. Regasini, F. Cotinguiba, G.D. Passerini, V.d.S. Bolzani, R.M. Barretto Cicarelli, M.J. Kato, M. Furlan, Braz. J. Pharmacogn. 19 (2009) 199.

[14] F.M.J. Vallet, US Pat. 3,910,959, 1975.

[15] J. Laane, J. Phys. Chem. 104A (2000) 7715.

[16] W. Caminati, S. Melandri, G. Corbelli, L.B. Favero, R. Meyer, Mol. Phys. 80 (1993) 1297.

[17] L.A. Leal, J.L. Alonso, D.G. Lister, J.C. Lopez, Mol. Phys. 81 (1994) 1205.

[18] C.Y. Panicker, H.T. Varghese, Y.S. Mary, Oriental J. Chem. 28 (2012) 1037.

[19] J. Laane, E. Bondoc, S. Sakurai, K. Morris, N. Meinander, J. Choo, J. Am. Chem. Soc. 122 (2000) 2628.

[20] S. Sakurai, N. Meinander, K. Morris, J. Laane, J. Am. Chem. Soc. 121 (1999) 5056.

[21] J.A. Duckett, T.L. Smithson, H. Wieser, Chem. Phys. Lett. 64 (1979) 261.

[22] H.-Kun Fun, C.K. Quah, M.I. Attia, M.F. El-Behairy, O.A. Al-Deeb, Acta Cryst. E68 (2012) o634.

[23] Gaussian 09, Revision B.01, M.J. Frisch, G.W. Trucks, H.B. Schlegel, G.E. Scuseria, M.A. Robb, J.R. Cheeseman, G. Scalmani, V. Barone, B. Mennucci, G.A. Petersson, H. Nakatsuji, M. Caricato, X. Li, H.P. Hratchian, A.F. Izmaylov, J. Bloino, G. Zheng, J.L. Sonnenberg, M. Hada, M. Ehara, K. Toyota, R. Fukuda, J. Hasegawa, M. Ishida, T. Nakajima, Y. Honda, O. Kitao, H. Nakai, T. Vreven, J.A. Montgomery, Jr., J.E. Peralta, F. Ogliaro, M. Bearpark, J.J. Heyd, E. Brothers, K.N. Kudin, V.N. Staroverov, T. Keith, R. Kobayashi, J. Normand, K. Raghavachari, A. Rendell, J.C. Burant, S.S. Iyengar, J. Tomasi, M. Cossi, N. Rega, J.M. Millam, M. Klene, J.E. Knox, J.B.

Cross, V. Bakken, C. Adamo, J. Jaramillo, R. Gomperts, R.E. Stratmann, O. Yazyev, A.J. Austin, R. Cammi, C. Pomelli, J.W. Ochterski, R.L. Martin, K. Morokuma, V.G. Zakrzewski, G.A. Voth, P. Salvador, J.J. Dannenberg, S. Dapprich, A.D. Daniels, O. Farkas, J.B. Foresman, J.V. Ortiz, J. Cioslowski, D.J. Fox, Gaussian, Inc., Wallingford CT, 2010.

[24] J.B. Foresman, in: E. Frisch (Ed.), Exploring Chemistry with Electronic Structure Methods; A Guide to Using Gaussian, Pittsburg, PA, 1996.

[25] A. Irfan, R. Jin, A.G. Al-Sehemi, A.M. Asiri, Spectrochim. Acta A 110 (2013) 60.

[26] P.J. Hay, W.R. Wadt, J. Chem. Phys. 82 (1985) 270.

[27] J.Y. Zhao, Y. Zhang, L.G. Zhu, J. Mol. Struct. Theochem. 671 (2004) 179.

[28] R. Dennington, T. Keith, J. Millam, GaussView, Version 5, Semichem Inc., Shawnee Mission, KS, 2009.

[29] J.M.L. Martin, C.V. Alsenoy, GAR2PED, A Program to Obtain a Potential Energy Distribution from a Gaussian Archive Record, University of Antwerp, Belgium, 2007.

[30] P. Sykes, A Guide Book to Mechanism in Organic Chemistry, sixth. ed., Pearson Education, India, New Delhi, 2004.

[31] K.B. Benzon, H.T. Varghese, C.Y. Panicker, K. Pradhan, B.K. Tiwary, A.K. Nanda, C. Van Alsenoy, Spectrochim. Acta A 151 (2015) 965.

[32] R.T. Ulahannan, C.Y. Panicker, H.T. Varghese, C. Van Alsenoy, R. Musiol, J. Jampilk, P.L. Anto, Spectrochim. Acta A 121 (2014) 404.

[33] N.P.G. Roeges, A Guide to the Complete Interpretation of Infrared Spectra of Organic Structures, John Wiley and Sons Inc., New York, 1994.

[34] G. Varsanyi, Assignments of Vibrational Spectra of Seven Hundred Benzene Derivatives, Wiley, New York 1974.

[35] Y.S. Mary, H.T. Varghese, C.Y. Panicker, T. Ertan, I. Yildiz, O.T. Arpaci, Spectrochim. Acta A 71 (2008) 566.

[36] M.K. Mishra, D.P. Pandey, Oriental J. Chem. 27 (2011) 305.

[37] A. Bigotto, B. Pergolese, J. Raman Spectrosc. 32 (2001) 953.

[38] N.B. Colthup, L.H. Daly, S.E. Wiberly, Introduction to Infrared and Raman Spectroscopy, Academic Press, Boston, 1990.

[39] G. Socrates, Infrared Characteristic Group Frequencies, John Wiley and Sons, New York 1981.

[40] C. Adant, M. Dupuis, J.L. Bredas, Int. J. Quantum. Chem. 56 (2004) 497.

[41] C. Hätting, O. Christiansen, P. Jørgensen, Chem. Phys. Lett. 282 (1998) 139.

[42] A.R. Katritzky, V.S. Lobanov, M. Karelson, Chem. Soc. Rev. 24 (1995) 279.

[43] R.J. Parr, R.G. Pearson, J. Am. Chem. Soc. 105 (1983) 7512.

[44] J.S. Murray, K. Sen, Molecular Electrostatic potentials, concepts and applications, Elsevier, Amsterdam, 1996.

[45] I. Alkorta, J.J. Perez, Int. J. Quant. Chem. 57 (1996) 123.

[46] E. Scrocco, J. Tomasi, in: P. Lowdin (Ed.), Advances in Quantum Chemistry, Academic Press, New York, 1978.

[47] F.J. Luque, M. Orosco, P.K. Bhadane, S.R. Gadre, J. Phys. Chem. 97 (1993) 9380.

[48] J. Sponer, P. Hobza, Int. J. Quant. Chem. 57 (1996) 959.

[49] A.E. Reed, R.B. Weinhold, J. Chem. Phys. 83 (1985) 735.

[50] R.G. Parr, W. Yang, Functional Theory of Atoms and Molecules, Oxford University Press, New York, 198.

[51] P.W. Ayers, R.G. Parr, J. Am. Chem. Soc. 122 (2000) 2010.

[52] R.G. Parr, W.J. Yang, Am. Chem. Soc. 106 (1984) 511.

[53] C. Morell, A. Grand, A. T. Labbe, J. Phys. Chem. A 109 (2005) 205.

[54] E.D. Glendening, A.E. Reed, J.E. Carpenter, F. Weinhold, NBO Version 3.1, Gaussian Inc., Pittsburgh, PA, 2003.

[55] S.H. Landis, T. Murray, S. Bolden, P.A. Wingo, Cancer J. Clin. 48 (1998) 6.

[56] H. Ohtsu, Z. Xiao, J. Ishida, M. Nagai, H.K. Wang, H. Itokawa, C.Y. Su, C. Shih, T. Chiang, E. Chang, Y.F. Lee, M.Y. Tsai, C. Chang, K.H. Lee, J. Med. Chem. 45 (2002) 5037.

[57] Z. Nahleh, Cancer Therapy 6 (2008) 439.

[58] Z. Nahleh, Future Oncol. 4(2008) 15.

[59] I.B.D. Kapelle, T.T. Irawadi, M.S. Rusli, D. Mangunwidjaja, Z.A. Masud, Cancer Res. J. 3 (2015) 68.

[60] O. Trott, A. J. Olson, J. Comput. Chem. 31 (2010) 455.

[61] B. Kramer, M. Rarey, T. Lengauer, Proteins: Struct. Funct. Genet. 37 (1999) 228.

Figure captions

Fig. 1: FT-IR spectrum of (*E*)-1-(1,3-benzodioxol-5-yl)-4,4-dimethylpent-1-en-3-one

Fig. 2: FT-Raman spectrum of (*E*)-1-(1,3-benzodioxol-5-yl)-4,4-dimethylpent-1-en-3-one

Fig. 3: Optimized geometry of (*E*)-1-(1,3-benzodioxol-5-yl)-4,4-dimethylpent-1-en-3-one

Fig. 4: HOMO-LUMO plots of (*E*)-1-(1,3-benzodioxol-5-yl)-4,4-dimethylpent-1-en-3-one

Fig. 5: MEP plot of (*E*)-1-(1,3-benzodioxol-5-yl)-4,4-dimethylpent-1-en-3-one

Fig. 6: The interactive plot of ligand and androgen receptor

Fig. 7: The docked protocol reproduced the co-crystallized conformation wth H-bond (green), π-alkyl (pink), π-π (magenta) and H-bond receptor surface shown

Fig. 8: Schematic for the docked conformation of active site of the title compound at androgen receptor

Table 1

Calculated (scaled) wavenumbers, observed IR, Raman bands and assignments of the title compound

B3LYP/SDD (6D, 10F)			IR	Raman	Assignments[a]
υ(cm^{-1})	IR_I	R_A	υ(cm^{-1})	υ(cm^{-1})	-
3126	4.00	173.60	-	3124	υCHPh(99)
3123	4.94	2.44	-	-	υCHPh(97)
3089	15.97	31.34	-	-	υCH(17), υCHPh(81)
3087	6.76	36.63	3085	-	υCH(79), υCHPh(17)
3056	29.35	135.86	-	-	υCH_2(100)
3052	0.24	26.12	-	-	υCH(97)
3030	38.20	57.43	-	-	υCH_3(98)
3018	78.27	162.26	3020	3018	υCH_3(92)
3014	73.15	53.80	-	-	υCH_3(96)
3010	9.39	14.08	-	-	υCH_3(98)
3007	48.84	88.41	-	-	υCH_3(90)
3004	4.84	11.17	-	-	υCH_3(100)
2979	126.06	283.00	2976	2973	υCH_2(100)
2932	40.06	330.81	-	-	υCH_2(42), υCH_3(46)
2922	21.90	185.13	-	-	υCH_3(94)
2920	33.71	4.39	2921	2922	υCH_3(98)
1625	185.52	1026.73	-	1624	υC=O(54), υC=C(13)
1599	9.31	626.31	1605	1595	υPh(68)
1581	20.57	102.84	1585	-	υPh(66)
1535	323.29	1956.98	1523	1540	υC=C(59), υC=O(12)
1479	50.59	6.16	1481	1482	δCH_3(85)
1475	7.05	38.31	-	-	δCH_2(91)
1468	18.20	21.35	-	-	δCH_3(86)
1463	162.90	26.41	-	-	δCHPh(27), υPh(54)
1463	9.43	20.07	-	-	δCH_3(89)
1452	0.78	16.57	-	-	δCH_3(92)

1450	0.02	15.05	1450	1450	δCH_3(90)
1442	0.59	2.91	-	-	δCH_3(92)
1425	208.45	386.20	-	1419	υPh(48), δCHPh(21)
1398	37.24	37.98	1396	-	δCH_3(92)
1375	14.99	1.43	-	-	δCH_3(94)
1371	14.92	0.27	1369	1370	δCH_3(96)
1359	46.30	8.66	-	-	υPh(47), δCH_2(16)
1354	9.20	51.71	-	-	δCH_2(67)
1309	6.38	180.74	1308	1308	δCH(57), υPh(22)
1296	28.45	10.16	-	-	δCH(18), υCC(15), δCHPh(17), υPh(10)
1254	8.94	0.69	1258	1256	δCHPh(50), δCH_3(28)
1239	38.87	81.69	1240	-	υCC(57), δCH_3(12)
1225	319.43	156.60	1222	-	δCH(47), υCO(21), υPh(10)
1204	10.53	5.04	-	-	υCC(49), δCH_3(20)
1187	6.21	7.28	1191	1188	δCH_3(25), υCC(47)
1180	43.12	7.94	-	-	δCHPh(43), υCO(13), υCC(11)
1117	47.32	13.68	1120	-	δCHPh(47), υPh(26)
1116	0.01	8.39	-	1114	δCH_2(99)
1070	159.90	60.87	1072	1072	υCC(34), δPh(20), δCH_3(15)
1059	6.30	1.39	-	-	δCH_2(99)
1047	71.45	135.17	1045	1045	δPh(32), υCO(50)
1020	29.80	6.03	1018	1019	γCH(43), τC=C(22)
1004	10.58	3.82	-	-	δCH_3(56), γCH(11)
999	96.32	66.08	-	-	δCH_3(63), υCC(18)
974	161.25	4.07	977	-	υCO(72), γCHPh(11)
949	3.60	0.99	-	951	γCHPh(82)
943	0.01	0.19	939	940	δCH_3(81)
923	6.45	2.92	-	-	υCC(13), υPh(10), δCH_3(46)
920	0.70	15.69	-	-	υCC(19), δCH_3(48)

911	3.48	5.87	-	-	υCC(46), δCH_3(40)
892	0.52	8.87	-	-	γCHPh(24), γCH(59)
880	22.78	4.16	882	-	γCHPh(63), γCH(12)
863	15.33	9.72	-	-	υCC(13), υCO(47)
850	51.16	6.56	-	860	υCO(72), γCHPh(12)
824	51.94	0.45	830	828	γCHPh(84)
791	1.95	5.36	792	-	υCC(45), δPh(11)
769	7.35	47.01	764	766	υPh(49), υCO(20), δPh(13)
732	2.66	0.31	733	735	τPh(60), γCC(11), γC=O(10)
725	4.36	5.21	-	722	δCO(29), δPh(33)
701	0.18	0.17	-	-	γC=O(30), τPh(29)
676	0.26	11.75	-	-	δCO(59), δPh(11)
597	6.76	0.35	-	-	γCC(32), τPh(43), τCO(12)
594	0.63	10.93	592	593	τCO(31), δPh(25)
560	0.34	17.13	-	-	δCC(45), δC=O(15)
511	21.16	1.15	518	515	δPh(10), δCC(50), δC=O(11)
497	12.41	3.77	-	-	δPh(46), δCC(19)
430	4.65	0.41	-	-	δPh(18), δCC(48)
426	4.91	0.20	428	424	τPh(26), δCH_2(30)
368	0.27	0.23	-	367	δCC(62), τPh(18)
368	5.11	1.02	-	367	δCC(39), δPh(26)
355	0.01	2.90	-	-	τPh(66)
340	7.09	0.71	-	-	δCC(62), δC=O(16)
293	7.58	3.02	-	-	δCC(75)
278	0.90	0.26	-	-	δCC(61), γC=O(13)
232	0.04	1.49	-	-	τPh(50), τCO(21)
224	0.32	0.70	-	-	τCH_3(92)
219	0.06	0.61	-	215	τCH_3(69)
203	0.08	0.16	-	-	τPh(51), τCO(14), τCH_2(20)
199	0.08	2.85	-	197	δC=C(17), δCC(39), δPh(11), τCH_2(22)

173	0.33	2.68	-	170	δCC(65), δC=C(11)
150	0.10	0.04	-	-	τCH_3(89)
116	0.10	2.73	-	118	τCC(28), γC=O(26), δCC(14)
69	5.74	0.10	-	-	τCC(20), τCO(21), γCC(11), τCH_2(39)
55	0.39	1.13	-	-	δCC(65), δC=C(28)
32	0.45	1.17	-	-	τCO(59), τCC(14)
29	15.15	2.17	-	-	τCO(87)
18	0.22	1.29	-	-	τCO(54), τCC(18)

[a]υ-stretching; δ-in-plane deformation; γ-out-of-plane deformation;τ -torsion; Ph-phenyl ring; potential energy distribution (%) is given in brackets in the assignment column; IRI-IR intensity; R_A-Raman activity.

Table 2

Second-order perturbation theory analysis of Fock matrix in NBO basis corresponding to the intramolecular bonds of the title compound.

Donor(i)	Type	ED/e	Acceptor(j)	Type	ED/e	E(2)[a]	E(j)-E(i)[b]	F(ij)[c]
O1-C7	σ	1.98871	C5-C6	σ*	0.02124	5.30	1.41	0.077
O2-C7	σ	1.98901	C8-C9	σ*	0.01923	5.18	1.42	0.077
C5-C6	π	1.68487	C4-C10	π*	0.37659	19.45	0.30	0.070
-	-	-	C8-C9	σ*	0.01923	19.32	0.30	0.068
C6-C8	σ	1.97755	C5-C6	σ*	0.02124	4.24	1.31	0.066
-	-	-	C8-C9	σ*	0.01923	4.46	1.32	0.069
C8-C9	π	1.72057	C4-C10	π*	0.37659	17.09	0.31	0.066
-	-	-	C5-C6	π*	0.37275	19.58	0.30	0.070
C12-C13	σ	1.98108	C10-C11	σ*	0.02179	4.25	1.15	0.062
-	-	-	C11-C12	σ*	0.01296	2.71	1.31	0.053
-	-	-	C14-C15	σ*	0.01795	1.33	1.04	0.033
C13-C14	σ	1.97304	C11-C12	σ*	0.01296	1.68	1.26	0.041
LPO1	σ	1.96172	O2-C7	σ*	0.02923	3.83	0.85	0.051
-	-	-	C6-C8	σ*	0.03996	4.25	1.14	0.062
-	π	1.84600	C5-C6	π*	0.37275	28.81	0.35	0.096
LPO2	σ	1.96105	O1-C7	σ*	0.03074	3.94	0.84	0.051
-	-	-	C6-C8	σ*	0.03996	4.14	1.13	0.061
-	π	1.85769	C8-C9	π*	0.34340	27.81	0.36	0.094
LPO3	σ	1.97714	C12-C13	σ*	0.05902	1.91	1.12	0.042
-	-	-	C13-C14	σ*	0.07527	1.67	1.05	0.038
-	π	1.88474	C12-C13	σ*	0.05902	19.52	0.70	0.106
-	-	-	C13-C14	σ*	0.07527	21.20	0.63	0.104

[a]E(2) means energy of hyper-conjugative interactions (stabilization energy in kJ/mol)

[b]Energy difference (a.u) between donor and acceptor i and j NBO orbitals

[c]F(i,j) is the Fock matrix elements (a.u) between i and j NBO orbitals

Table 3

NBO results showing the formation of Lewis and non-Lewis orbitals.

Bond(A-B)	ED/e[a]	EDA%	EDB%	NBO	s%	p%
σO1-C7	1.98871	68.21	31.79	0.8259($sp^{2.90}$)O+	25.63	74.37
-	-0.82137	-	-	0.5638($sp^{3.68}$)C	21.30	78.70
σ O2-C7	1.98901	68.05	31.95	0.8249($sp^{2.88}$)O+	25.78	74.22
-	-0.82302	-	-	0.5653($sp^{3.63}$)C	21.52	78.48
π C5-C6	1.68487	51.47	48.53	0.7174($sp^{1.00}$)C+	0.00	100.0
-	-0.27165	-	-	0.6966($sp^{1.00}$)C	0.00	100.0
σ C6-C8	1.97755	49.99	50.01	0.7070($sp^{1.91}$)C+	34.39	65.61
-	-0.72263	-	-	0.7072($sp^{1.92}$)C	34.29	65.71
π C8-C9	1.72057	49.55	50.45	0.7039($sp^{1.00}$)C+	0.00	100.0
-	-0.27320	-	-	0.7103($sp^{1.00}$)C	0.00	100.0
σ C12-C13	1.98108	51.64	48.36	0.7186($sp^{2.09}$)C+	32.38	67.62
-	-0.64307	-	-	0.6954($sp^{1.87}$)C	34.81	65.19
σ C13-C14	1.97304	48.05	51.95	0.6932($sp^{1.84}$)C+	35.16	64.84
-	-0.59757	-	-	0.7207($sp^{3.15}$)C	24.09	75.91
n1O1	1.96172	-	-	$sp^{1.36}$	42.34	57.66
-	-0.60055	-	-	-	-	-
n2O1	1.84600	-	-	$sp^{1.00}$	0.00	100.0
-	-0.33106	-	-	-	-	-
n1O2	1.96105	-	-	$sp^{1.35}$	42.55	57.45
-	-0.59875	-	-	-	-	-
n2O2	1.85769	-	-	$sp^{1.00}$	0.00	100.0
-	-0.32875	-	-	-	-	-
n1O3	1.97714	-	-	$sp^{0.77}$	56.37	43.63
-	-0.66104	-	-	-	-	-
n2O3	1.88474	-	-	$sp^{1.00}$	0.00	100.0
-	-0.24018	-	-	-	-	-

[a]ED/e in a.u.

Table 4

The binding affinity values of different poses of the title compound predicted by Autodock Vina.

Mode	Affinity (kcal/mol)	Distance from best mode (Å)	
-	-	RMSD l.b.	RMSD u.b.
1	-8.1	0.000	0.000
2	-7.6	1.015	2.107
3	-7.3	1.559	7.080
4	-7.1	1.380	7.097
5	-5.6	12.701	13.823
6	-5.5	1.456	6.988
7	-5.5	12.910	13.830
8	-5.1	12.770	14.309
9	-5.1	10.130	11.672

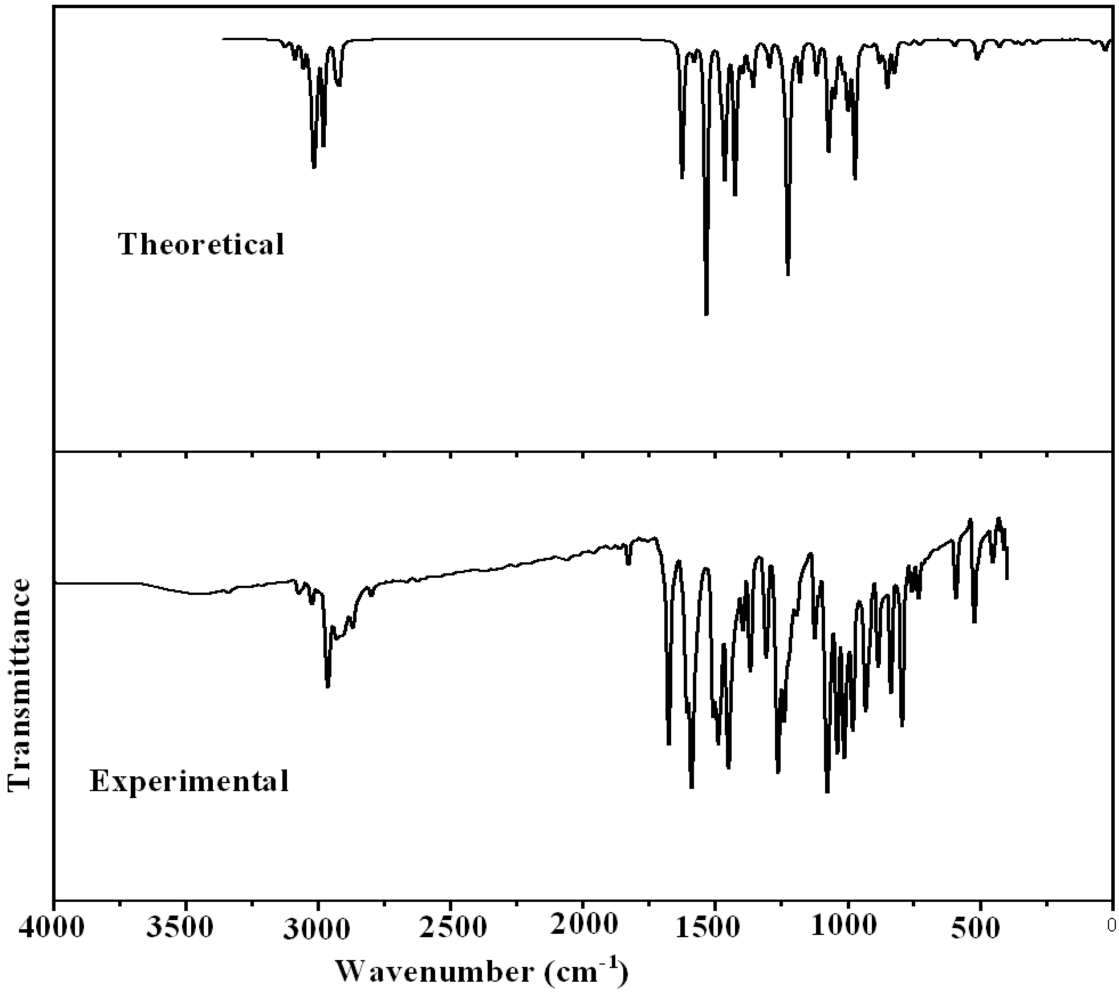

Fig.1 FT-IR spectrum of (E)-1-(1,3-Benzodioxol-5-yl)-4,4-dimethylpent-1-en- 3-one

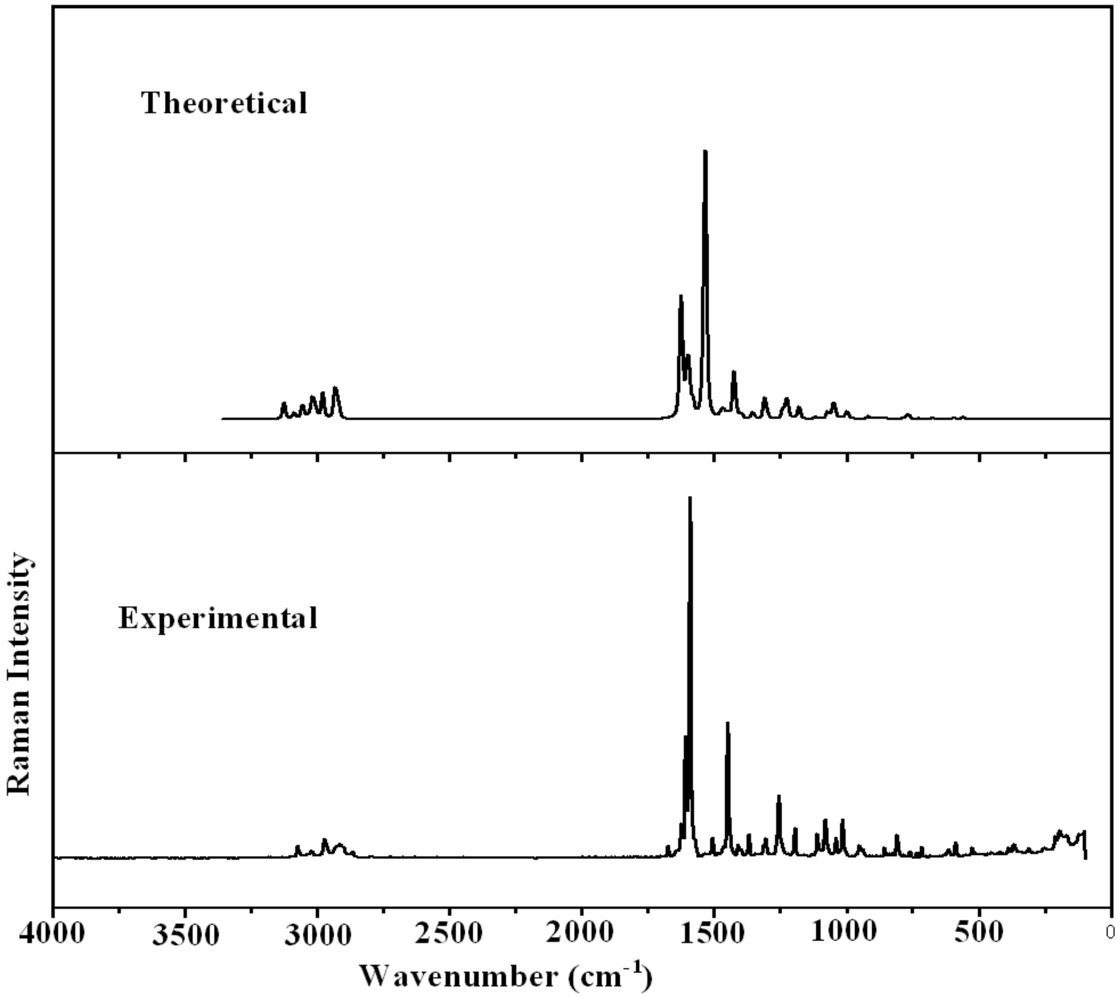

Fig.2 FT-Raman spectrum of

(E)-1-(1,3-Benzodioxol-5-yl)-4,4-dimethylpent-1-en-3-one

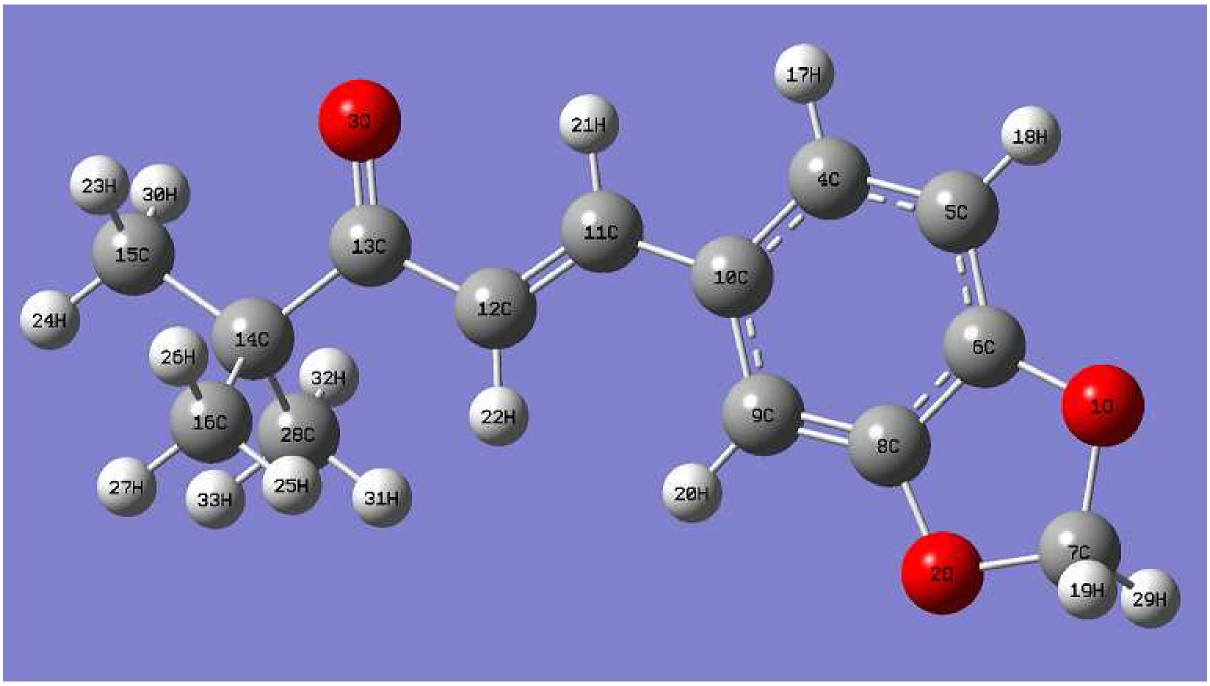

Fig.3 Optimized geometry of

(E)-1-(1,3-Benzodioxol-5-yl)-4,4-dimethylpent-1-en-3-one

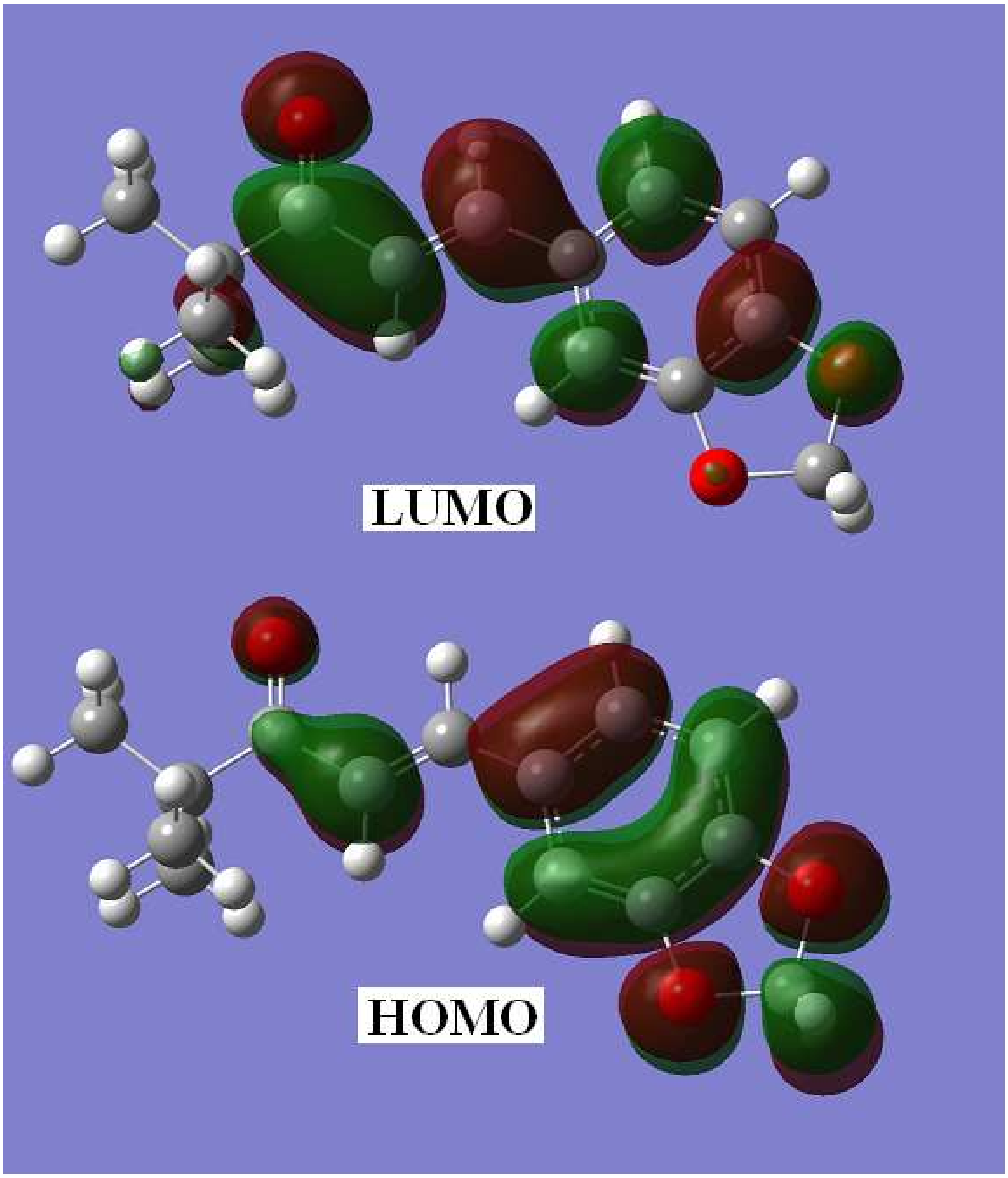

Fig.4 HOMO-LUMO plots of (E)-1-(1,3-Benzodioxol-5-yl)-4,4-dimethylpent-1-en-3-one

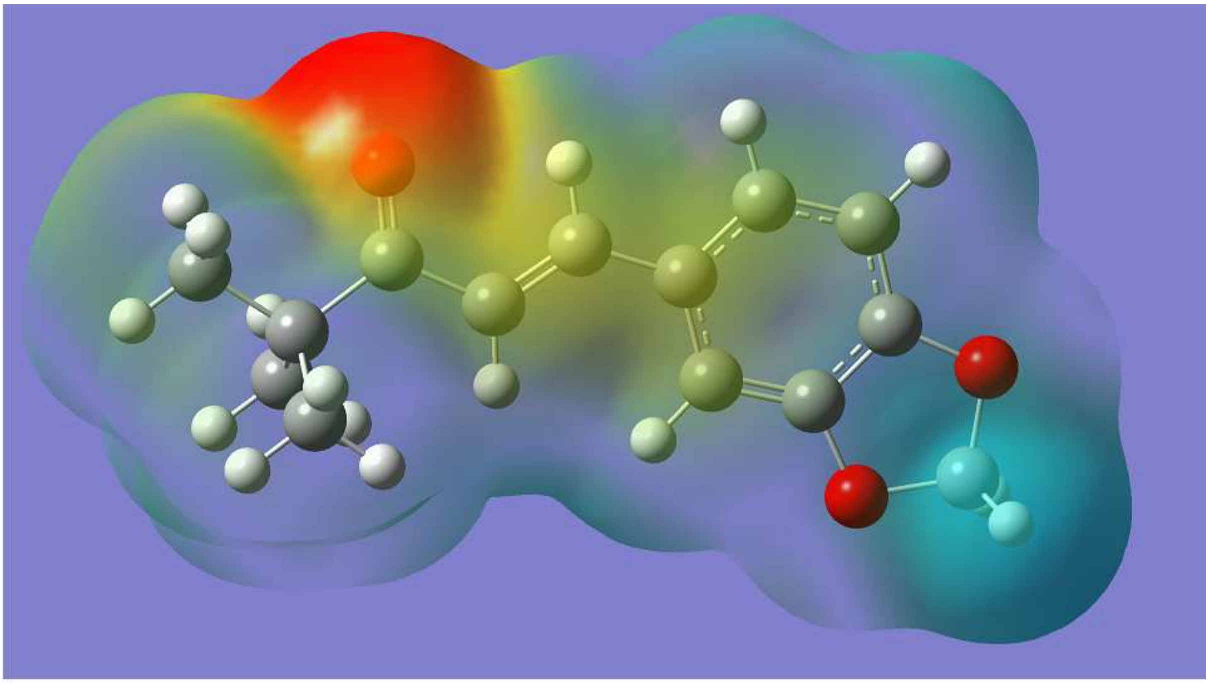

Fig.5 MEP plot of (E)-1-(1,3-Benzodioxol-5-yl)-4,4-dimethylpent-1-en-3-one

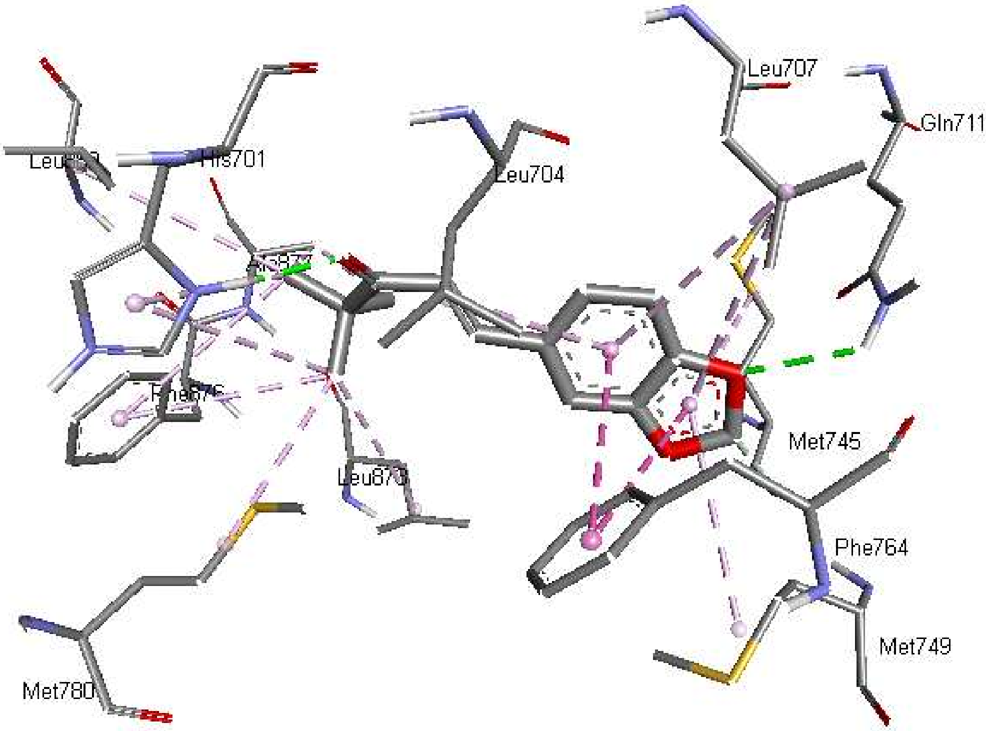

Fig.6 The interactive plot of ligand and androgen receptor

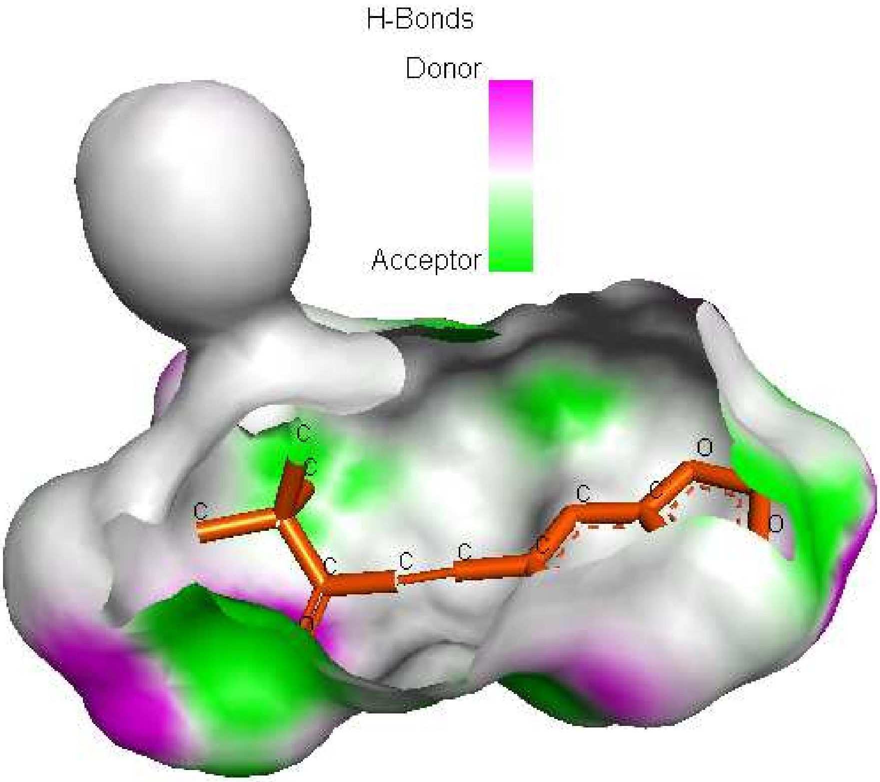

Fig.7 The docked protocol reproduced the co-crystallized conformation wth H-bond (green), π-alkyl (pink), π-π (magenta) and H-bond receptor surface shown

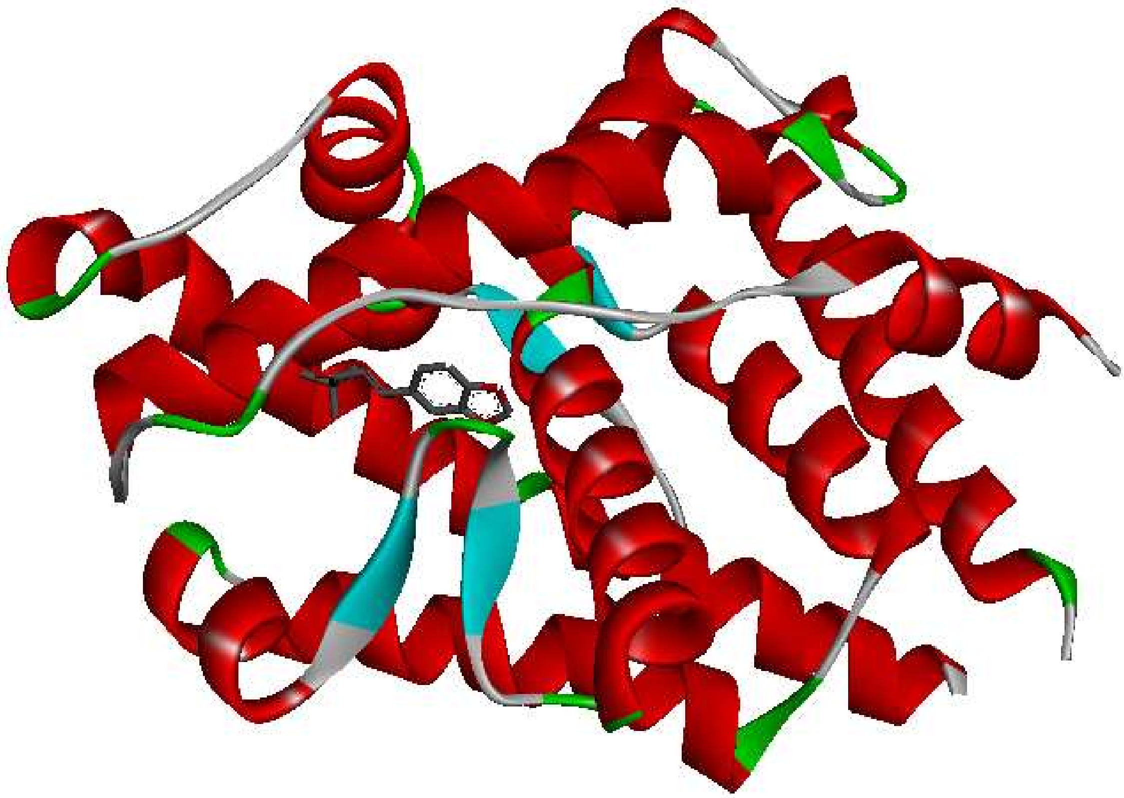

Fig.8 Schematic for the docked conformation of active site of the title compound at androgen receptor

Highlights

* IR, Raman spectra, Fukui functions, MEP, NLO and NBO analysis were reported.
* The wavenumbers are calculated theoretically using Gaussian09 software.
* The geometrical parameters are in agreement with the XRD data.
* Molecular docking the results suggest that the compound might exhibit inhibitory activity against androgen receptor.